JVSTA Journal of Vacuum Science & Technology A

Epitaxial niobium dioxide thin films by reactive-biased target ion beam deposition

Yuhan Wang, Ryan B. Comes, Salinporn Kittiwatanakul, Stuart A. Wolf, and Jiwei Lu

Citation: Journal of Vacuum Science & Technology A **33**, 021516 (2015); doi: 10.1116/1.4906143
View online: http://dx.doi.org/10.1116/1.4906143
View Table of Contents: http://scitation.aip.org/content/avs/journal/jvsta/33/2?ver=pdfcov
Published by the AVS: Science & Technology of Materials, Interfaces, and Processing

Epitaxial niobium dioxide thin films by reactive-biased target ion beam deposition

Yuhan Wang[a)]
Department of Materials Science and Engineering, University of Virginia, Charlottesville, Virginia 22904

Ryan B. Comes
Fundamental and Computational Sciences Directorate, Pacific Northwest National Laboratory, Richland, Washington 99352

Salinporn Kittiwatanakul
Department of Materials Science and Engineering, University of Virginia, Charlottesville, Virginia 22904

Stuart A. Wolf
Department of Materials Science and Engineering and Department of Physics, University of Virginia, Charlottesville, Virginia 22904

Jiwei Lu
Department of Materials Science and Engineering, University of Virginia, Charlottesville, Virginia 22904

(Received 31 October 2014; accepted 6 January 2015; published 16 January 2015)

Epitaxial NbO_2 thin films were synthesized on Al_2O_3 (0001) substrates via reactive bias target ion beam deposition. X-ray diffraction and Raman spectra were used to confirm the tetragonal phase of pure NbO_2. Through XPS, it was found that there was a ~1.3 nm thick Nb_2O_5 layer on the surface and the bulk of the thin film was NbO_2. The epitaxial relationship between the NbO_2 film and the substrate was determined. Electrical transport measurement was measured up to 400 K, and the conduction mechanism was discussed. © *2015 American Vacuum Society*.
[http://dx.doi.org/10.1116/1.4906143]

I. INTRODUCTION

Niobium dioxide (NbO_2) undergoes a metal–insulator transition (MIT) with rapid changes in resistivity and magnetic susceptibility and a simultaneous structural transition from a distorted rutile structure (space group $I4_1/a$) to a rutile structure (space group $P4_2/mnm$) at ~1081 K.[1–4] The transition behaviors of NbO_2 have much in common with that of vanadium dioxide (VO_2),[5] but the transition temperature of NbO_2 is much higher than that of VO_2 (~340 K), which makes it less susceptible to Joule heating and therefore more appealing in circuit applications. Besides the temperature-induced MIT, it has been reported that the MIT in NbO_2 could also be triggered by applied electrical field,[6–9] that makes it attractive as a switching material. The electrically induced transition showed threshold characteristics and monostable switching devices have been fabricated using NbO_2 films, which can be potentially applied as nanoelectronic devices.[6,8] Despite the attractive attributes of NbO_2, experimental studies on NbO_2—especially NbO_2 thin films—has remained limited due to the difficulty in preparing high quality NbO_2 films. Preparation of NbO_2 films has being challenging because Nb^{4+} is not a stable oxidation state of niobium and is easily over-oxidized. In previous studies, amorphous and polycrystalline NbO_2 films have been prepared by sputtering a NbO_2 target reduced from Nb_2O_5,[10] by the chemical vapor transport method,[11] or dc magnetron sputtering.[12] Recently, epitaxial NbO_2 thin films have been prepared by DC reactive sputtering and MBE growth.[13,14]

In this paper, we investigated the synthesis of epitaxial NbO_2 thin films using the reactive bias target ion beam deposition (RBTIBD) process. The RBTIBD process utilizes a beam ion source to produce a very high density of low energy (5–50 eV) inert gas ions,[15] and the deposition has been described in detail previously.[16] Reactive gases (e.g., oxygen and nitrogen) can be mixed with the inert gas in a precise and controlled manner to react with the sputtered metal atoms and form the desired compound. The key advantage of the RBTIBD technique is the ability to precisely control adatom energies, which controls composition and phase formation and offers the ability to operate in a rather wide processing window.[16,17] The technique has been used to synthesize high quality epitaxial VO_2 films on various kinds of substrates.[16,18,19]

II. EXPERIMENT

RBTIBD, as mentioned above, was used to deposit the NbO_2 films. The main chamber was pumped down to a base pressure of $\sim 9 \times 10^{-8}$ Torr before each deposition. The films were deposited on 430 μm Al_2O_3 (0001) substrates. The niobium target with 99.99% purity was sputtered using an Ar/O_2 80/20 mixture that also supplied the oxygen. The Nb target was water-cooled during the deposition. The stage heater was ramped up to 500 °C at a rate of ~20 °C/min and allowed to stabilize for 45 min. The ion sources were initiated using a 10 SCCM Ar gas flow and 7 A for the cathode and 70 SCCM Ar gas flow and 6 A for the anode. The substrates were precleaned in low energy Ar ions (~50 eV) for 3 min with the wafer carrier rotating at a speed of 10 rpm. A pulsed dc potential bias was applied to the target with a

a)Electronic mail: yw9ep@virginia.edu

negative bias of −900 V and positive bias of +20 V at a frequency of 71.34 kHz and a positive duty cycle of 3 μs. The target was presputtered for 15 min with the stage shutter closed to clean the target surface, while the reactive Ar/O_2 mixture was set to the desired flow rate and allowed to stabilize. Then the stage shutter was opened and the films were deposited for 30 min. The process pressure was around 1.2×10^{-3} Torr during the deposition. The growth condition parameters including optimized growth temperature and Ar/O_2 flow rates for the samples in this study are listed in Table I.

The film thicknesses were determined by x-ray reflectivity (Smart Lab, Rigaku Inc.), and the one reported here was around 110 nm thick. X-ray diffraction (XRD) scans of 2θ were performed in a range from 20° to 100° to investigate the phase composition of the films and the rocking curve was measured to characterize the crystallinity. The orientation relationship between the NbO_2 film and the sapphire substrate was determined by in-plane ϕ scan. Raman spectra were measured with an inVia Raman microscope (Renishaw systems Ltd.) using a 514 nm laser source at 50% power. Surface morphology was characterized by atomic force microscopy (AFM) (Cypher®, Asylum Research, Inc.), and the images were processed using software Gywddion. XPS measurements were performed using a VG Scienta R3000 system with monochromated Al Kα radiation with base pressure of 1×10^{-9} Torr. The resistivity was measured using the four-point probe method in a temperature range from 185 to 400 K.

III. RESULTS AND DISCUSSION

Figure 1(a) shows the out-of-plane 2θ scan of a NbO_2 film grown on a (0001) sapphire substrate. The diffraction peaks from the thin film were observed at 2θ of 37.18° and 79.21°. The peak at $2\theta = 41.63°$ and $2\theta = 90.65°$ corresponds to (0006) plane and (00012) plane of sapphire substrate, respectively. The thin film peaks correspond to (440) and (880) in the low temperature phase NbO_2 (distorted rutile structure), indicating not only a single-phase but also highly textured NbO_2 thin film. There are clear Kiessig fringes observed in the scan as seen in the inset of Fig. 1(a), which are indicative of the high quality epitaxy of the NbO_2 film with abrupt interfaces, uniform thickness, and low defect density. The lattice parameter "a" was ~13.67 Å based on the 2θ values of diffraction peaks from NbO_2. The lattice spacing is very close to that of single crystal NbO_2 (13.70 Å),[2] and it implies that the film strain is fully relaxed. The in-plane lattice mismatch between the NbO_2 film and the substrate is calculated to be ~−1.2%. Based on a formula simplified from Matthews and Blakeslee's equation,[20] the critical thickness is ~20 nm, above which dislocations would form to release the misfit epitaxial strain in the film. Given the film thickness of ~110 nm, the epitaxial strain is expected to be fully relaxed, which is in good agreement with the experimental observation.

To characterize the crystallinity of the NbO_2 film, the rocking curves, i.e., ω scan were measured for the (440) reflection of the NbO_2 film and the (0006) reflection of the

TABLE I. Optimized growth parameter for single phase NbO_2 via RBTIBD.

Substrate temperature	500 °C
Process pressure	9×10^{-4} Torr
Ar/O_2 80/20 mix flow rate	5.5 SCCM
Target potential bias	−900 and +20 V
DC pulse frequency	71.43 kHz
Positive duty cycle	3 μs
Cathode Ar flow rate and current	10 SCCM and 7 A
Anode Ar flow rate and current	70 SCCM and 6 A

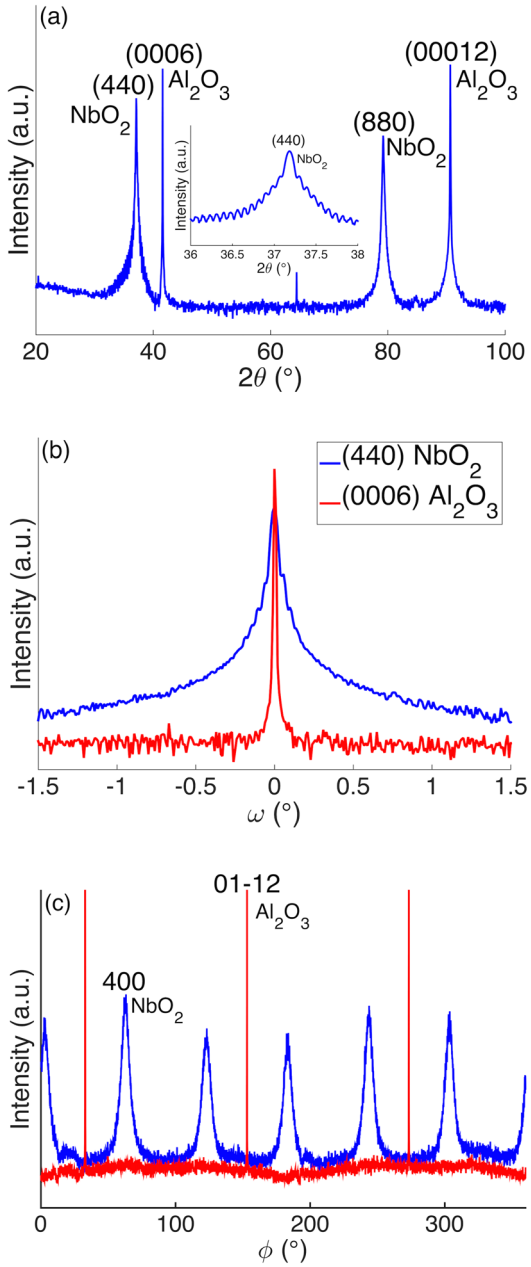

FIG. 1. (Color online) (a) 2θ scan of NbO_2 film deposited on (0001) sapphire substrate, inset shows 2θ scan of (440) diffraction peak of NbO_2; (b) ω scan of (440) of NbO_2 and (0006) of sapphire substrate; (c) In-plan ϕ scan of (400) ($2\theta = 26°$ and $\chi = 45°$) of NbO_2 (top) and ($01\bar{1}2$) ($2\theta = 25.5°$ and $\chi = 12.8°$) of sapphire substrate (bottom).

sapphire substrate as shown in Fig. 1(b). Kiessig fringes were also visible in the rocking curve. The peaks have been fitted to extract the full width at half maximum (FWHM). The FWHM for (440) NbO_2 was 0.042°. For comparison, FWHM for (0006) of the single crystal sapphire substrate is 0.0093°. Previous studies reported the FWHM of ~0.07° for (200) NbO_2 grown on a (111) single crystal $(La,Sr)_2(Al,Ta)_2O_6$ substrate using molecular beam epitaxy[13] and the FWHM of 0.18° for (440) NbO_2 grown on a (0001) single crystal sapphire substrate using DC magnetron reactive sputtering.[14] The smaller FWHM of the (440) NbO_2 peak observed here indicates that the defect density is significantly reduced, which is attributed to the unique capability of the bias target ion beam technique.[16–19]

X-ray ϕ scans were performed on (400) NbO_2 diffraction peaks at $2\theta = 26°$ and $\chi = 45°$ and $(01\bar{1}2)$ Al_2O_3 diffraction peaks at $2\theta = 25.5°$ and $\chi = 12.8°$, which are shown in Fig. 1(c). The presence of six diffraction peaks from the (400) NbO_2 indicates that there are three equivalent orientations in the basal plane. While the NbO_2 film has only one out of plane orientation, three in plane variants rotate 120° from each other in the basal plane. Also shown in Fig. 1(c), the off-axis NbO_2 (400) peaks and Al_2O_3 $(01\bar{1}2)$ peaks are offset by 30°. The c-plane of sapphire has three-fold symmetry, and the structure of NbO_2 deposited on top is tetragonal. As a result, the crystals of NbO_2 can have three preferred in-plane orientations in accordance to the substrate and film crystal structures. The same in-plane textures were observed in VO_2 grown on c-plane sapphire substrates.[21] Combining in-plane and out-of-plane XRD spectra, the epitaxial relationship between the film and the substrate can be summarized as $\langle 100\rangle(110)NbO_2 \| \langle 10\bar{1}0\rangle(0001)Al_2O_3$, which is in good agreement with the previous report.[14]

An AFM image of the NbO_2 film is shown in Fig. 2. This image was scanned using tapping mode at a scan rate of 1 Hz. The film appears to be very smooth, with a root mean square (RMS) roughness of ~0.12 nm. There are no cracks or pinholes observed on a large $20 \times 20\,\mu m^2$ area. The smooth morphology of the film surface is due to the fact that the substrate was directly exposed to the ion beam that was used for the sputtering.[16] The ion beam can provide additional kinetic energies for the adatoms on the surface, which results in very smooth surfaces in crystallized oxide thin films. According to the applied voltage of ion source, this additional kinetic energy was ~50 eV, which was not enough to cause the sputtering of NbO_2 films on the substrate but could modify the surface morphology as reported in previous studies.[17,22]

Figure 3 shows the Raman spectra of the 110 nm thick NbO_2 thin film on the sapphire substrate measured with a 514 nm laser source. The measured spectrum contained the background from the substrate, and the spectrum with the contribution from the substrate subtracted is also shown in Fig. 3 for comparison. To the best of our knowledge, there are no reported Raman spectra of bulk single crystal NbO_2. The Raman spectrum agreed well with the previous reports on the Raman spectra of NbO_2 films.[11,23,24] No Raman shifts corresponding to Nb_2O_5,[25,26] which is the most stable niobium oxide, were observed. The result indicates that the film mainly consists of the tetragonal NbO_2 phase, within the limitations of the Raman tool.

Core level Nb 3d spectra were acquired using XPS to characterize the oxidation state of the film surface and near surface portions of the film. The valence band density of states was also measured. Both measurements are shown in Fig. 4. The Nb 3d level is shown in Fig. 4(a) with measurements made both before and after the sputter removal of surface carbon and oxide layers formed in the ambient conditions. The primary peak between 207 and 208 eV at normal emission corresponds to Nb^{5+}, with a small Nb^{4+} peak between 205 and 206 eV. Using angle-resolved measurements where the depth sensitivity is governed by the formula

$$I(z) = I_0 e^{-z/\lambda}, \tag{1}$$

where λ is the electron inelastic mean free path, z is the depth in the sample, and I_0 is the emission intensity at zero depth, we can determine if the over-oxidation to Nb^{5+} is limited to the surface. We assume a value of λ of 20 Å based on published values for Nb metal and Al_2O_3 at the relevant binding energies.[27] By tilting the sample so that the photoelectron emission comes from a glancing angle of 20° with a total integrated probe depth for 95% of the signal of approximately 16 Å, we observe that the Nb^{4+} peak is almost completely absent, indicating that the films are over-oxidized at the surface in ambient conditions. The bulk of the film must

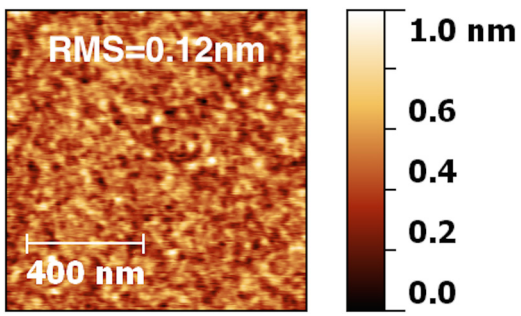

FIG. 2. (Color online) AFM image of a 110 nm thick NbO_2 film deposited on (0001) sapphire substrate. The root mean square (rms) surface roughness was ~0.12 nm.

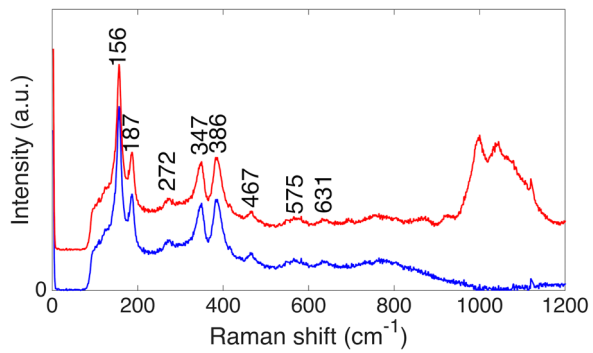

FIG. 3. (Color online) Raman spectra of NbO_2 deposited on the sapphire substrate at room temperature excited with a 514 nm laser source. The spectrum at the bottom is after subtracting the background from the substrate.

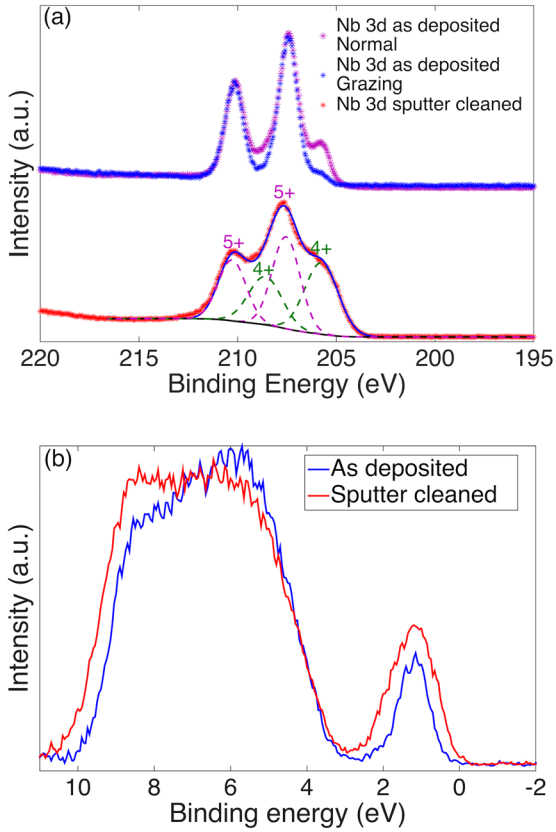

FIG. 4. (Color online) (a) (Top) Core level Nb 3d spectra obtained at incidence angles of 20° vs 90°. (Bottom) Normal emission after sputter cleaning and (b) valence band XPS spectra of a NbO_2 film deposited on (0001) sapphire. The grazing incidence (20°) probes exclusively the surface layer.

therefore have a significantly greater Nb^{4+} intensity, while the surface is exclusively Nb^{5+}.

To characterize the film below the surface, the surface layer was removed using *in situ* ion beam sputtering with 500 eV Ar^+ ions and the XPS measurements were repeated. The peaks were fitted using a constrained model of the $3d^{5/2}$ and $3d^{3/2}$ peaks based on a 3:2 branching ratio between the spin-orbit split peaks. The Nb^{4+} peak is found to be 48% of the overall signal, suggesting a significant amount of Nb^{5+} remains in the sample after sputter cleaning. Tilting to 20° emission again showed a reduction in the Nb^{4+} peak intensity to nearly zero intensity. These results suggest that even in ultrahigh vacuum conditions that the surface will readily oxidize to Nb^{5+} by scavenging any available O_2 or H_2O. If we assume that the surface of the film is exclusively Nb^{5+} for the first 13 Å of depth after sputtering and exclusively Nb^{4+} for lower depths, then the integrated relative intensities of the Nb^{4+} and Nb^{5+} peaks should be 48% and 52%, respectively. This suggests that an ~13 Å thick layer of disordered Nb_2O_5 is present on the surface even in extremely low oxygen pressures. A similar result has been observed elsewhere in NbO_2 films.[24] From this, we can conclude that the bulk of the film is Nb^{4+}, but that the surface is highly unstable. Attempts to reduce the surface from Nb^{5+} through *in situ* vacuum annealing did not succeed and actually increased the Nb^{5+} peak intensity relative to Nb^{4+}, presumably due to greater reaction kinetics at high temperatures with the scavenged O_2 and H_2O molecules. Valence band spectra shown in Fig. 4(b) confirm that there is significant intensity of Nb 4d electrons at lower binding energies above the edge of the O 2p band, in agreement with other works.[24]

Figure 5 shows the temperature dependence of the electrical resistivity of the NbO_2 film from 185 to 400 K. The resistivity of the NbO_2 film was ~0.2 Ω·cm at 400 K, and then increased several orders of magnitude to ~400 Ω·cm at 185 K. Below 185 K, the resistance of the sample was beyond the measurement limit of the instrument. The room temperature resistivity reported here is comparable to that of thin films,[24] but is much lower than that of bulk samples,[28,29] which can be attributed to the higher defect concentrations in the thin film than in the single crystal.

To understand the conduction mechanism in NbO_2, the temperature dependence of the resistivity was fitted to Mott's variable range hopping (VRH) model[30] and the Efros–Shklovskii model,[31] respectively. Mott's VRH model was used to describe the conduction mechanisms in thin film VO_2 and Cr doped VO_2,[16,32] in which the density of states near Fermi level varies slowly with energy and electron–electron interaction is neglected. In comparison the Efros–Shklovskii VRH model describes the conduction in materials, in which the Coulomb interaction leads to a depression of DOS near Fermi level, giving rise to a Coulomb gap.[33] The crossover from Mott's VRH model to Efros–Shklovskii VRH model has been observed in semiconductors such as amorphous indium oxide and CdSe.[34,35] The fitting results show that Efros–Shklovskii variable range hopping model described the conduction mechanism in NbO_2 better; however, the discrepancy between experimental data and model becomes appreciable above room temperature, and this can be caused by the transition of the conduction mechanism from the hopping of small polarons to the band conduction in an intrinsic semiconductor as the temperature increases as reported for the single crystal NbO_2 samples.[28,29] To fully elucidate the conduction mechanisms in the NbO_2 film, transport measurements need to be

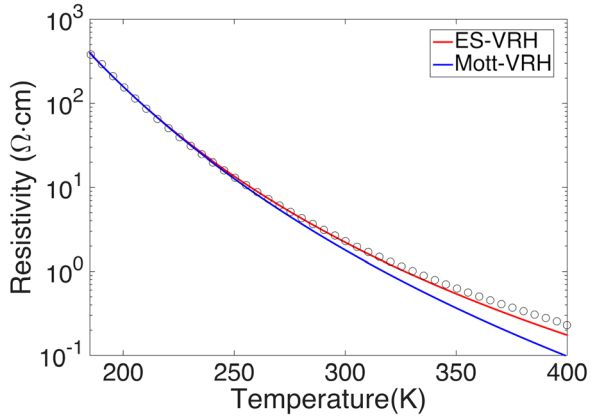

FIG. 5. (Color online) Resistivity vs temperature for a 110 nm thick NbO_2. The solid lines are the fittings using the Mott's variable range hopping (VRH) and Efros–Shklovskii (ES-VRH) models.

conducted at elevated temperatures up to the metal–insulator transition temperature (1081 K for bulk NbO_2).

IV. CONCLUSIONS

In summary, epitaxial NbO_2 films were successfully deposited on (0001) Al_2O_3 substrates using the RBTIBD technique. No secondary phases of niobium oxides were observed in XRD. The FWHM of the rocking curve for (440) NbO_2 was 0.042°. The epitaxial orientation relationship between NbO_2 film and substrate was $\langle 100\rangle(110)NbO_2 \parallel \langle 10\bar{1}0\rangle(0001)Al_2O_3$. The film surface was remarkably smooth with an RMS roughness of ~0.12 nm. Raman spectra confirm the phase pure tetragonal NbO_2, and no features of other oxides were observed. The oxidation state of Nb^{4+} was further confirmed by XPS, in which the presence of a thin Nb_2O_5 layer (~1.3 nm) was also observed at the surface due to the oxidation of NbO_2 in the ambient environment. Finally, the resistivity was measured from 185 to 400 K and can be described by the Efros–Shklovskii variable range hopping model.

ACKNOWLEDGMENTS

R.B.C. was supported by the Linus Pauling Distinguished Postdoctoral Fellowship at Pacific Northwest National Laboratory (PNNL LDRD PN13100/2581). The PNNL work was performed in the Environmental Molecular Sciences Laboratory, a national science user facility sponsored by the Department of Energy's Office of Biological and Environmental Research and located at Pacific Northwest National Laboratory.

[1]R. F. Janninck and D. H. Whitmore, J. Phys. Chem. Solids **27**, 1183 (1966).
[2]A. A. Bolzan, C. Fong, B. J. Kennedy, and C. J. Howard, J. Solid State Chem. **113**, 9 (1994).
[3]A. K. Cheetham and C. N. R. Rao, Acta Crystallogr., Sect. B **32**, 1579 (1976).
[4]R. Pynn, J. D. Axe, and R. Thomas, Phys. Rev. B **13**, 2965 (1976).
[5]V. Eyert, Europhys. Lett. **58**, 851 (2002).
[6]S. Kim *et al.*, Microelectron. Eng. **107**, 33 (2013).
[7]J. C. Lee and W. W. Durand, J. Appl. Phys. **56**, 3350 (1984).
[8]M. D. Pickett and R. S. Williams, Nanotechnology **23**, 215202 (2012).
[9]H. R. Philipp and L. M. Levinson, J. Appl. Phys. **50**, 4814 (1979).
[10]J. M. Gallego and C. B. Thomas, Thin Solid Films **98**, 11 (1982).
[11]S. Lee, H. Yoon, I. Yoon, and B. Kim, Bull. Korean Chem. Soc. **33**, 839 (2012).
[12]X. Liu, S. M. Sadaf, S. Kim, K. P. Biju, X. Cao, M. Son, S. H. Choudhury, G. Y. Jung, and H. Hwang, ECS Solid State Lett. **1**, Q35 (2012).
[13]A. B. Posadas, A. O'Hara, S. Rangan, R. A. Bartynski, and A. A. Demkov, Appl. Phys. Lett. **104**, 092901 (2014).
[14]F. J. Wong and S. Ramanathan, J. Mater. Res. **28**, 2555 (2013).
[15]H. R. Kaufman, R. S. Robinson, and R. I. Seddon, J. Vac. Sci. Technol., A **5**, 2081 (1987).
[16]K. G. West, J. W. Lu, J. Yu, D. Kirkwood, W. Chen, Y. H. Pei, J. Claassen, and S. A. Wolf, J. Vac. Sci. Technol., A **26**, 133 (2008).
[17]J. J. Quan, S. A. Wolf, and H. N. G. Wadley, J. Appl. Phys. **101**, 074302 (2007).
[18]J. W. Lu, K. G. West, and S. A. Wolf, Appl. Phys. Lett. **93**, 262107 (2008).
[19]S. Kittiwatanakul, J. W. Lu, and S. A. Wolf, Appl. Phys. Express **4**, 091104 (2011).
[20]J. W. Matthews and A. E. Blakeslee, J. Cryst. Growth **27**, 118 (1974).
[21]L. Wang, E. Radue, S. Kittiwatanakul, C. Clavero, J. Lu, S. A. Wolf, I. Novikova, and R. A. Lukaszew, Opt. Lett. **37**, 4335 (2012).
[22]W. Chen, D. N. H. Nam, J. Lu, K. G. West, and S. A. Wolf, J. Appl. Phys. **106**, 013905 (2009).
[23]Y. Zhao, Z. Zhang, and Y. Lin, J. Phys. D: Appl. Phys. **37**, 3392 (2004).
[24]F. J. Wong, N. Hong, and S. Ramanathan, Phys. Rev. B **90**, 115135 (2014).
[25]B. X. Huang, K. Wang, J. S. Church, and Y. S. Li, Electrochim. Acta **44**, 2571 (1999).
[26]A. A. Mcconnell, J. S. Anderson, and C. N. R. Rao, Spectrochim. Acta, Part A **32**, 1067 (1976).
[27]S. Tanuma, C. J. Powell, and D. R. Penn, Surf. Interface Anal. **11**, 577 (1988).
[28]G. Bélanger, J. Destry, G. Perluzzo, and P. M. Raccah, Can. J. Phys. **52**, 2272 (1974).
[29]Y. Sakai, N. Tsuda, and T. Sakata, J. Phys. Soc. Jpn. **54**, 1514 (1985).
[30]N. F. S. Mott, *Electronic Processes in Non-crystalline Materials*, edited by N. F. Mott and E. A. Davis (Clarendon, Oxford, 1971), pp. 39–49.
[31]A. L. Efros and B. I. Shklovskii, J. Phys. C: Solid State **8**, L49 (1975).
[32]K. G. West *et al.*, J. Supercond. Novel Magn. **21**, 87 (2008).
[33]W. N. Shafarman, D. W. Koon, and T. G. Castner, Phys. Rev. B **40**, 1216 (1989).
[34]R. Rosenbaum, Phys. Rev. B **44**, 3599 (1991).
[35]Y. Z. Zhang, P. H. Dai, M. Levy, and M. P. Sarachik, Phys. Rev. Lett. **64**, 2687 (1990).